

Anomalous behaviors of the charge and spin degrees of freedom in the CuO double chains of $\text{PrBa}_2\text{Cu}_4\text{O}_8$

S. Nishimoto

Philipps-Universität Marburg, Fachbereich Physik, D-35032 Marburg, Germany

Y. Ohta^y

Department of Physics, Chiba University, Chiba 263-8522, Japan

(dated: March 22, 2024)

The density-matrix renormalization-group method is used to study the electronic states of a two-chain Hubbard model for CuO double chains of $\text{PrBa}_2\text{Cu}_4\text{O}_8$. We show that the model at quarter filling has the charge ordered phases with stripe-type and in-line (type patterns in the parameter space, and in-between, there appears a wide region of vanishing charge gap; the latter phase is characteristic of either Tomonaga-Luttinger liquid or a metallic state with a spin gap. We argue that the low-energy electronic state of the CuO double chains of $\text{PrBa}_2\text{Cu}_4\text{O}_8$ should be in the metallic state with a possibly small spin gap.

PACS numbers: 71.10.Fd, 71.30.+h, 71.10.Hf, 75.40.Mg, 71.27.+a

I. INTRODUCTION

Geometrical frustration in the charge degrees of freedom of the CuO double chains of $\text{PrBa}_2\text{Cu}_4\text{O}_8$ has provided an interesting opportunity for studying anomalous metallic states realized in quasi-one-dimensional (1D) electronic conductors. Experimentally, it has been reported^{1,2,3} that the system shows metallic conductivity along the chain direction down to 2K and that it shows insulating conductivity along the directions perpendicular to the chain above 140 K. The system may thus be regarded as a quasi-1D correlated conductor except at low temperatures. Below 140 K, the conductivity of the system shows a 2D behavior within the crystallographic a-b plane,² indicating that the coupling between the chains is not negligible.

Anomalous behaviors in $\text{PrBa}_2\text{Cu}_4\text{O}_8$ have been observed in particular in its charge degrees of freedom. A nuclear-quadrupole-resonance (NQR) experiment⁴ showed that the temperature dependence of the spin-lattice ($1=T_1$) and spin-spin ($1=T_2$) relaxations is anomalous, indicating the presence of very slow fluctuations of charge carriers. A polarized optical spectrum for E_ka (electric field E parallel to the a axis) demonstrated that the CuO_2 planes of this material maintain the charge-transfer (CT) insulating state with a CT gap of 1.4 eV,^{5,6} which is typical of that of cuprates, but the spectrum for E_kb (chain direction) exhibits a broad peak structure at $\omega > 40$ meV with a very small but nonzero D₀ weight ($\sim 2\%$ of the total weight)⁵. Tomonaga-Luttinger liquid (TLL) behavior was also suggested; from the power-law dependence dominating in the higher-energy part of the optical conductivity, the exponent K was estimated to be 0.24 ⁵. Moreover, an angle-resolved photoemission spectroscopy (ARPES) study of Zn-doped $\text{PrBa}_2\text{Cu}_4\text{O}_8$ showed a power-law behavior of the spectral function near the Fermi level, which is indicative of a TLL state, and a value $K \sim 0.24$ was

estimated.^{7,8} Such a small value of K suggests that the long-range Coulomb interaction between charge carriers should be very strong. It was also reported that the system of the CuO double chains is near quarter filling of holes.^{5,7} A good opportunity has thus been provided for studying the anomalous charge dynamics of strongly correlated 1D electron systems such as charge ordering (CO), charge fluctuation, and charge frustration.

A few theoretical studies have so far been made on the CuO double chains of $\text{PrBa}_2\text{Cu}_4\text{O}_8$. Using Lanczos exact-diagonalization technique on small clusters, Seo and Ogata⁹ studied similar models and proposed possibility of the appearance of a metallic phase due to geometrical frustration; the system sizes used were however very small, so that whether the first charge excitation is gapped or gapless in the thermodynamic limit was not clear. Zhuravlev et al.¹⁰ investigated a spinless Fermion model at half filling, which corresponds to a quarter-filled extended Hubbard model in the limit of large on-site repulsion U , and found that a metallic state is realized due to the effect of frustration among Fermions when long-range repulsive interactions among them compete. Amasaki et al.¹¹ calculated the optical conductivity spectrum in the mean-field theory and showed that it agrees well with experiment only when the stripe-type CO is present; they thereby argued that the observed anomalous optical response may be due to the presence of the stripe-type fluctuations of charge carriers in the CuO double chains.

Motivated by such development in the field, we here investigate the ground state of the extended Hubbard model at quarter filling, an effective model for the CuO double chain of $\text{PrBa}_2\text{Cu}_4\text{O}_8$. An isolated double-chain system is considered in this paper because to clarify its nature is essential before the dimensional crossover⁷ is taken into account. We use the density-matrix renormalization-group (DMRG) method¹² for calculating the ground and low-energy excited states of the model, as well as its charge and spin correlation func-

tions.

We will show that our model in its ground state has the CO phases with stripe-type and in-line (type patterns in the parameter space, and in-between, there appears a wide region of vanishing charge gap; the latter phase is characteristic of either a TLL or a metallic state with a spin gap. The spin gap remains open unless the filling deviates largely from a quarter. We will then consider possible experimental relevance of our results. We will in particular argue that the low-energy electronic state of the CuO double chains of $\text{PrBa}_2\text{Cu}_4\text{O}_8$ show metallic state with a possibly small spin gap.

This paper is organized as follows. In Sec. I we introduce a single-band Hubbard model defined on a 1D lattice for the CuO double chain of $\text{PrBa}_2\text{Cu}_4\text{O}_8$ and give some numerical details of the DMRG method used. In Sec. III, we present calculated results for the charge gap, phase diagram, spin correlations, charge correlations, and Luttinger parameters, and discuss anomalous properties of the liquid phase of our system. In Sec. IV, we summarize the results obtained and discuss their possible experimental relevance.

II. MODEL AND METHOD

The structural element of $\text{PrBa}_2\text{Cu}_4\text{O}_8$ that we consider is the CuO double chain with unit cell Cu_2O_4 ,^{1,2} the geometry of which is illustrated in Fig. 1 (a). The relevant orbitals on the Cu and O sites are the $3d_{x^2-y^2}$ and $2p$ orbitals, respectively. From the antibonding band of these two orbitals, we may extract an effective model, i.e., a single-band extended Hubbard model for low-energy electronic states of the CuO double chains (see Fig. 1 (b)), where the O ions are no longer explicitly present. Such reduction of dimensionality allows us to carry out detailed numerical studies. One should also note that this two-chain Hubbard model is topologically equivalent to the single-chain Hubbard model with next-nearest-neighbor interactions as shown in Fig. 1 (c).

The model we consider is thus described by the Hamiltonian

$$\begin{aligned}
 H = & \sum_i^X (c_{i+1}^\dagger + c_{i+1}^\dagger c_i) \\
 & + \sum_i^X (c_{i+2}^\dagger + c_{i+2}^\dagger c_i) \\
 & + U \sum_i n_{i\uparrow} n_{i\downarrow} \\
 & + V_1 \sum_i n_{i\uparrow} \frac{1}{2} n_{i+1\downarrow} + \frac{1}{2} \\
 & + V_2 \sum_i n_{i\uparrow} \frac{1}{2} n_{i+2\downarrow} + \frac{1}{2} \quad (1)
 \end{aligned}$$

where we use the notations for the 1D chain defined in Fig. 1 (c). c_i^\dagger (c_i) is the creation (annihilation) operator of a hole with spin (\uparrow, \downarrow) at site i and $n_i = c_i^\dagger c_i$ is

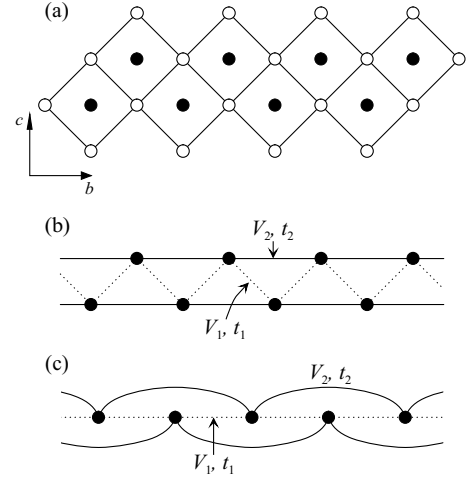


FIG. 1: (a) Schematic representation of the lattice structure of the CuO double chain. The solid circles represent Cu ($d_{x^2-y^2}$) orbitals and the open circles represent O (p) orbitals. (b) The corresponding two-chain Hubbard model. (c) Geometrically equivalent single-chain Hubbard model.

the number operator. t_1 and V_1 are the nearest-neighbor hopping integral and Coulombic repulsion, respectively, which are for the zigzag bonds connecting two chains of the two-chain model (see Fig. 1 (b)). t_2 and V_2 are those for the next-nearest-neighbor bonds, which are for the chain bonds of the two-chain model. We assume $t_1 = t_2$ because of the bonding angle minimizing the overlap of the Cu $3d_{x^2-y^2}$ and O $2p$ wave functions for the hopping parameter t_1 ; in the following, we use the value $t_1 = t_2 = 0.1$ unless otherwise stated, by assuming that the sign of t_1 does not change the results. We assume a value of the on-site Coulomb interaction U as $U = t_2 = 20$, which is somewhat larger than a typical value for cuprate materials; by using this value, however, we can investigate interesting features of our model with a wide range of V_1 and V_2 . We believe that this choice does not change the essential features of our results. The filling of holes in the CuO double chains is reported to be $n = 0.5$ ^{5,7}; we therefore restrict ourselves to the case at quarter filling unless otherwise indicated, i.e., $n = \frac{1}{2}$ corresponding to a density of one hole per two Cu sites. Note that the repulsions V_1 and V_2 are frustrating interactions for the charge degrees of freedom of the system in the sense that two holes can choose to sit on two of the three sites of a triangle of the lattice in mutually competing energy scales V_1 and V_2 (see Fig. 1 (b)). If we assume the intersite Coulomb repulsions to be inversely proportional to the intersite distance, we have the relation $V_1 = 2V_2$, which is not far from the line $V_1 = 2V_2$ where the two repulsions V_1 and V_2 exactly compete at $t_1 = t_2 = 0$.

We use the DMRG method,¹² a powerful numerical technique for a variety of 1D systems, whereby we can obtain very accurate ground-state energies and expectation values for very large finite-size systems. We study the chains with up to 128 sites. The open-end boundary

conditions are used; when we calculate local quantities, they are actually the ones averaged over the chain and when we show correlation functions, they are the ones measured from the midpoint of the chain. We use up to $m = 2000$ density matrix eigenstates to build the DMRG basis. One needs to keep relatively large values of m to obtain sufficient accuracies in our system because the long-range hopping term increases the truncation error rapidly; this is in particular the case when $t_1 \neq 0$. Extrapolating the DMRG ground-state energies calculated for different m values to an energy for vanishing discarded weight,¹³ we obtain the ground state energy and excitation gap which are accurate to parts in $10^{-3} t_2$. Although the largest source of errors in our calculations are finite size effects, we are able to extrapolate a number of gap values measured for different system sizes to a value for an infinite system-size chain.

In the following, we first present calculated results for the charge gap in order to show that the geometrical frustration indeed induces the metal-insulator (MI) phase transition; the ground-state phase diagram is shown in the parameter space of the inter-site Coulomb interactions. We then present calculated results for the density distributions, spin-spin correlation functions, charge velocities, and the density-density correlation functions, in order to discuss possible anomalous behaviors of the metallic phase.

III. RESULTS OF CALCULATION

A. Charge gap

The charge gap of an L -site chain is defined by

$$\begin{aligned} \Delta_c(L) = & \frac{1}{2} E_0(N_\uparrow + 1; N_\downarrow + 1; L) \\ & + E_0(N_\uparrow - 1; N_\downarrow - 1; L) - 2E_0(N_\uparrow; N_\downarrow; L), \end{aligned} \quad (2)$$

where $E_0(N_\uparrow; N_\downarrow; L)$ denotes the ground-state energy of a chain of length L with N_\uparrow spin-up holes and N_\downarrow spin-down holes. In Fig. 2 (a), we show calculated results for $\Delta_c(L)/t_2$ at $V_1/t_2 = 5$ for several V_2/t_2 values and system sizes L up to 80 sites. We find that $\Delta_c(L)$ decreases monotonically with increasing L , so that we can extrapolate $\Delta_c(L)$ to the thermodynamic limit systematically by performing the least-square fit of $\Delta_c(L)$ to a second-order polynomial in $1/L$. The extrapolated results $\Delta_c(L \rightarrow \infty)/t_2 (= \Delta_c(L \rightarrow 1)/t_2)$ are shown in Fig. 2 (b). It is evident that for both small $V_2/t_2 < 1.56$ and large $V_2/t_2 > 5.95$, $\Delta_c(L \rightarrow \infty)/t_2$ is finite, i.e., the system is insulating, and in a wide range of V_2/t_2 , i.e., $1.56 < V_2/t_2 < 5.95$, $\Delta_c(L \rightarrow \infty)/t_2$ vanishes within the accuracy of the extrapolation. We find similar situations for other values of V_1/t_2 as well, which demonstrates that a stable metallic phase indeed exists between two insulating phases.

When $t_1 = t_2 = 0$, we readily find from a total-energy calculation that there are two ordered phases, of which

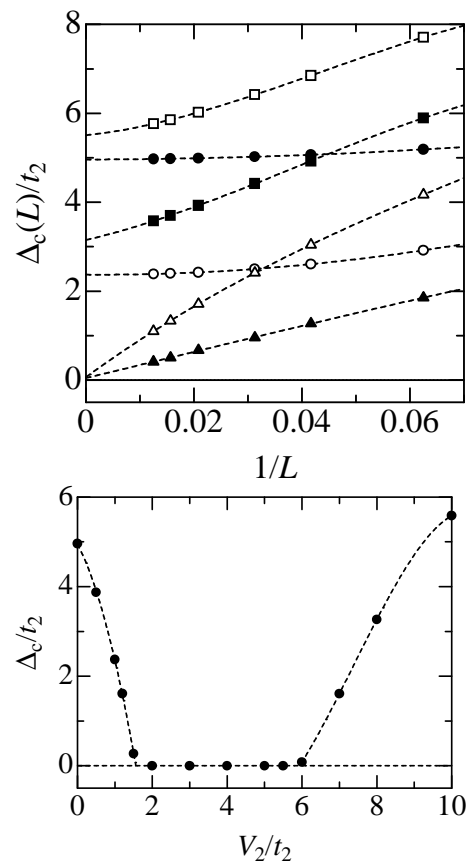


FIG. 2: Charge gap in the extended Hubbard model [Eq. (1)] at quarter filling for $V_1/t_2 = 5$ and $t_1/t_2 = 0.1$. (a) $\Delta_c(L)/t_2$ calculated as a function of the inverse system size $1/L$ for $V_2/t_2 = 0$ (filled circles), 1 (open circles), 2 (filled triangles), 6 (open triangles), 8 (filled squares), and 10 (open squares). Dashed lines are the quadratic fits in $1/L$. (b) V_2/t_2 dependence of Δ_c/t_2 in the thermodynamic limit $L \rightarrow \infty$. The circles show the results obtained by extrapolation of the DMRG data in (a). The dashed lines are a guide to the eye.

the phase boundary locates on a $V_1 = 2V_2$ line. The phase in the $V_1 > 2V_2$ region is characterized by an in-line CO, i.e., all the holes locate on one of the two chains of the two-chain model, whereas the phase in the $V_1 < 2V_2$ region is characterized by a stripe-type CO, i.e., holes locate alternately on sites of both of the two chains forming a stripe-like pattern along the chain direction. The stripe-type CO corresponds to the $2k_F$ charge-density-wave (CDW) state and the in-line CO corresponds to the $4k_F$ -CDW in the single-chain notation of Fig. 1 (c). Note that, if we assume the intersite Coulomb repulsion to be inversely proportional to the intersite distance, we have $V_1 = 2V_2$ and hence the stripe-type CO should be realized, but if we assume a faster decay of the intersite repulsion due to the effect of screening, the energies of the two phases can be more comparable.

By making t_1 and t_2 finite to introduce quantum fluctuations, there appears the metallic state between these two insulating phases, where the two intersite repulsions

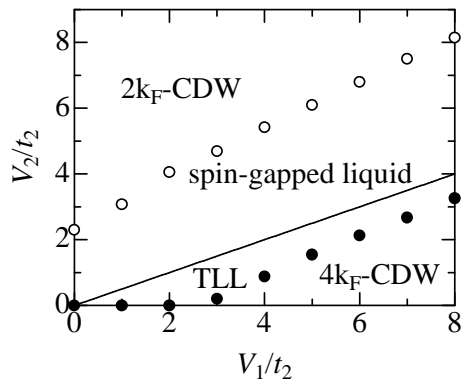


FIG. 3: Ground-state phase diagram of the model [Eq. (1)] in the parameter space of the intersite Coulomb interactions. The values $t_1 = 0.1t_2$ and $U = 20t_2$ are assumed. The open (solid) circles indicate the phase boundary between the $2k_F$ -CDW ($4k_F$ -CDW) and metallic states, at which the calculated charge gap ϵ_c vanishes. The solid line corresponds to $V_2=t_2 = V_1=(2t_2)$. Details of the metallic phase are discussed in Sec. III E.

V_1 and V_2 are mutually competing, as we have shown above. The ground-state phase diagram of our model (see Sec. III E for detailed discussion) therefore includes three phases in the parameter space as shown in Fig. 3; (i) the insulating phase with the $4k_F$ -CDW (or in-line CO) realized when V_1 is large, (ii) the insulating phase with the $2k_F$ -CDW (or stripe-type CO) realized when V_2 is large, and (iii) the metallic phase in-between. These three phases are discussed further in the following subsections.

B. Charge ordering

Let us first consider the three phases from the viewpoint of ordering of charge degrees of freedom. We first of all note that the CO is a state with a broken translational symmetry; there are two degenerate ground states, and in the open-end boundary conditions we use here, one of the two ground states is picked out by initial conditions of the calculation. The CO state is thus directly observable in our calculations.

For small values of $V_2=t_2$ ($< V_1=2t_2 = 0(t_2)$), the effect of $V_1=t_2$ dominates and leads to a CO with wave vector $q = 4k_F$ in the single-chain notation (which corresponds to the in-line type CO in the two-chain notation); namely, the ground state of the system is dominated by configurations such as

$$\dots 01010101010\dots,$$

where "1" stands for a site supporting one hole and "0" stands for an empty site. Fig. 4 (a) shows an example of the Friedel oscillation appeared in the density distribution $\langle n_i \rangle$ in the finite-size system of $L = 128$. One can see the $4k_F$ -CDW behavior clearly. The oscillations persist at the center of the chain and the difference between the

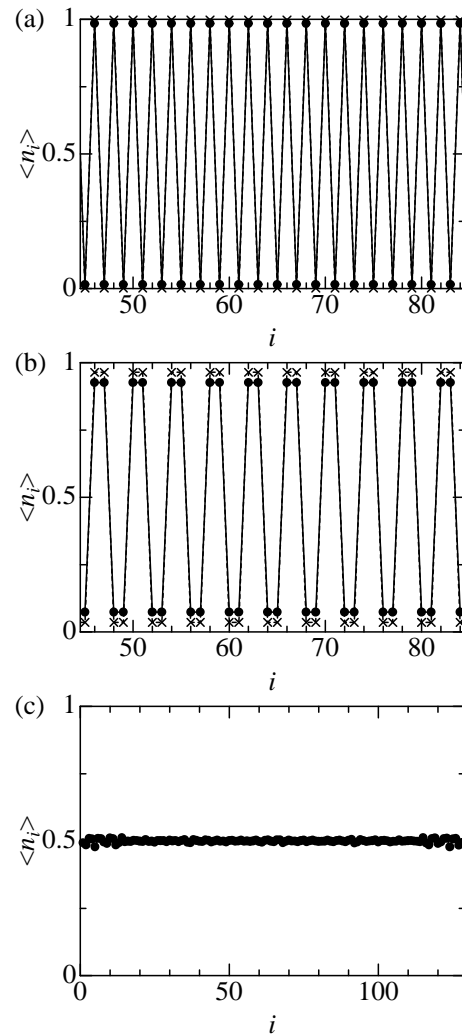


FIG. 4: Calculated hole densities at site i for (a) the $4k_F$ -CDW (or in-line type CO) at $V_2=t_2 = 0$ (crosses) and 1 (circles), (b) $2k_F$ -CDW (or stripe-type CO) at $V_2=t_2 = 6$ (circles) and 8 (crosses), and (c) uniform metallic phase at $V_2=t_2 = 2$. We assume $V_1=t_2 = 5$ and use the system of $L = 128$. Results for central 40 sites are shown in (a) and (b).

results for $V_2=t_2 = 0$ and 1 is hardly visible. We calculate $\langle n_{i+l} \rangle$ for several chain lengths and confirm that the system size with $L = 128$ is sufficiently large and the finite-size effect is negligible. We also calculate the density-density correlation function $N(l)$ defined as

$$N(l) = \langle n_{i+l} n_i - \langle n_{i+l} \rangle \langle n_i \rangle \rangle; \quad (3)$$

with $n_i = n_{i'} + n_{i\#}$ and find that $N(l)$ tends to a nonzero constant value as the intersite distance l increases: e.g., $N(l=1) \approx 10^{-7}$ at $V_1=t_2 = 5$ and $V_2=t_2 = 1$. This indicates the presence of the long-range ordered $4k_F$ -CDW state.

At $V_2=t_2 = 0$ where the $4k_F$ -CDW is stabilized, most of the charges are located on one of the two chains of the two-chain model although there are some charges on the other chain due to quantum fluctuation by a small value

of $t_1=t_2$; at $t_1=t_2=0$, the charges are disproportionated on one of the chains completely. With increasing $V_2=t_2$, the charge gap decreases rapidly (see Fig. 2 (b)), but the $4k_F$ -CDW correlation is hardly suppressed until reaching a sharp decline occurred around the MI transition point. This transition is of the second-order due to the presence of a small value of t_1 ; if $t_1=0$, this transition should be of the first-order. These results suggest that at $V_2=t_2 < 1.56$ and $V_1=t_2=5$ the system may be regarded as a half-filled extended Hubbard model since most of the charges are disproportionated. We note that, in the case of $t_1=1$ and $t_2=0$, the suppression of $4k_F$ -CDW correlation by V_2 has been suggested in the weak-coupling renormalization-group study.¹⁴

For large values of $V_2=t_2$ ($> V_1=2t_2 + O(t_1)$), $V_2=t_2$ enhances the $2k_F$ -CDW fluctuations and induces a CDW with wave vector $q=2k_F$ (or a stripe-type CO in the two-chain notation). The ground-state wave functions have dominant configurations of the type

$$\dots 011001100110\dots$$

where we use the same notations as above. Fig. 4 (b) shows an example of the Friedel oscillation appeared in the density distribution m_i in the finite-size system of $L=128$. The $2k_F$ -CDW behavior is clearly seen. The calculated values of $N(l)$ tends to a nonzero constant as the intersite distance l increases: e.g., $N(l=1) \approx 10^8$ at $V_1=t_2=5$ and $V_2=t_2=8$. This indicates the presence of long-range ordered $2k_F$ -CDW state.

When $V_2=t_2$ is much larger than $V_1=t_2$, $2k_F$ -CDW (or stripe-type CO) is stabilized, i.e., in the single-chain notation, two occupied sites and two empty sites come alternately. As shown in the next subsection, two spins on the neighboring two sites form a spin-singlet pair. As $V_2=t_2$ decreases, ρ_c decreases in proportion to $V_2=t_2$, and its behavior is similar to that of the model without hybridization ($t_1=t_2=0$); i.e., $\rho_c = 2(V_2 - V_2^{c;2k_F})$ around the MI transition point $V_2^{c;2k_F}$. This suggests that the charges disproportionated almost completely as soon as the charge gap opens. It can also be verified by slight reduction of the amplitude of the $2k_F$ -CDW oscillation that occurs when $V_2=t_2$ decreases. This means that the effect of $V_1=t_2$ directly weakens the effect of $V_2=t_2$ and melts the $2k_F$ -CDW state. This situation is similar to the MI transition of the quarter-filled extended Hubbard model. The transition is of the second order for $t_2 > 0$; it is of the first order only at $t_2 = 0$.

For intermediate values of $V_2=t_2$ (or around $V_1=2V_2$), the system is in the metallic state. As expected, the amplitude of the Friedel oscillation is quite small as shown in Fig. 4 (c), which should vanish at the center of the chain when $L \rightarrow 1$. In this phase, competition of two incompatible fluctuations, i.e., the $2k_F$ and $4k_F$ (or stripe-type and in-line type) charge fluctuations, prohibit the system from forming CO states. However, it is useful to know what is the dominant correlation; here, we examine the long distance behavior of the density-density correlations $N(l)$, in particular its period of oscillation. We thus find

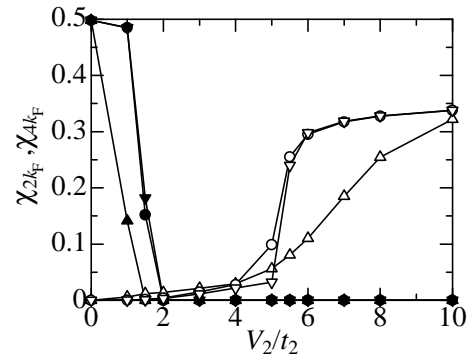


FIG. 5: Order parameters χ_{4k_F} and χ_{2k_F} as a function of $V_2=t_2$ for various system sizes at $V_1=t_2=1$. The filled (open) symbols are the results for χ_{4k_F} (χ_{2k_F}). The up-triangles, circles, and down-triangles denote the results for $L=16, 48,$ and 80 , respectively.

that the $2k_F$ CO correlation is dominant for $2V_2 > V_1$ and the $4k_F$ CO correlation is dominant for $2V_2 < V_1$, as will be discussed further in Sec. III D.

In order to explain relationship between the MI transition and CO formation, we introduce the order parameters defined as

$$\chi_{4k_F} = \frac{1}{L_e} \sum_j e^{i4k_F r_j} n_j = \frac{1}{L_e} \sum_j (-1)^j n_j \quad (4)$$

for the $4k_F$ -CDW and

$$\chi_{2k_F} = \frac{1}{L_e} \sum_j e^{i2k_F r_j} n_j = \frac{1}{L_e} \sum_j \cos \frac{j}{2} n_j; \quad (5)$$

for the $2k_F$ -CDW. Here, the sum is taken over central L_e ($=L-a$) sites excluding $a=2$ sites at both ends of the system in order to eliminate edge effects; here we take $a=8, 12$.

The obtained results at $V_1=t_2=5$ as a function of $V_2=t_2$ are shown in Fig. 5 for a number of system sizes. We find that as the system size increases the slopes of the curves around the critical points become steeper and that the result at $L=48$ is nearly equal to the result at $L=80$. Thus, the situation in the thermodynamic limit may well be expected except near the critical point where the size effect is not negligible. Let us focus on the $2k_F$ -CDW transition at $V_2=t_2 \approx 5.95$. Then, χ_{2k_F} shows a sharp development around $V_2=t_2 \approx 5$, which is rather smaller than the value of $V_2^{c;2k_F}=t_2$ shown in Fig. 2 (b). However, in the thermodynamic limit, this turning point should agree with $V_2^{c;2k_F}=t_2$, and the transition seems to be still continuous. We note that the transition becomes sharper for larger $V_1=t_2$ (or smaller t_2) values and is of the first-order in the limit $V_1 \rightarrow 1$ (or $t_2 \rightarrow 0$). A similar interpretation can also be given to the $4k_F$ -CDW transition.

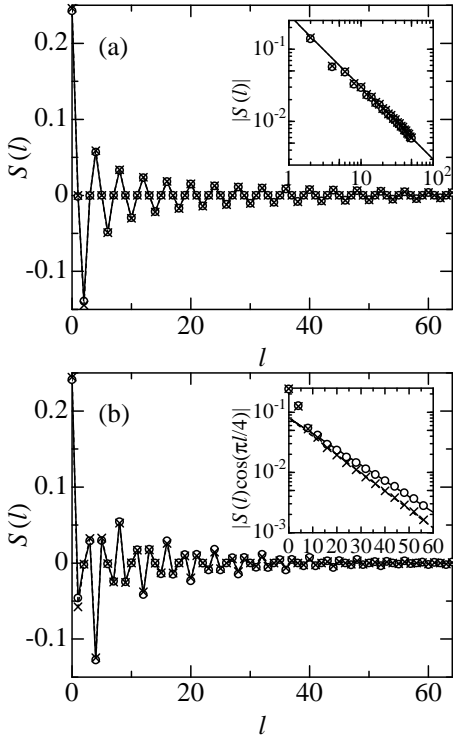


FIG. 6: (a) Spin-spin correlation function $S(l)$ as defined in Eq. (6) at $V_2=t_2 = 0$ (crosses) and 1 (circles) with $V_1=t_2 = 5$. The distance l is measured along the t_1 -chain in units of the interval between two sites. The log-log plot in the inset shows that the power-law decay of correlations. (b) $S(l)$ at $V_2=t_2 = 8$ (circles) and 10 (crosses) with $V_1=t_2 = 5$. The semi-log plot in the inset shows the exponential decay of correlations.

C. Spin correlations

In order to study the spin degrees of freedom of the system, we now calculate the spin-spin correlation function defined by

$$S(l) = S_1^z S_{i+1}^z; \quad (6)$$

with $S_i^z = (n_i - n_{i\#})/2$.

Let us first discuss the $4k_F$ -CDW phase (or in-line CO phase in the two-chain notation). Fig. 6(a) shows the spin-spin correlation functions calculated at $V_2=t_2 = 0$ and 1 with $V_1=t_2 = 5$ for the system of $L = 128$. The site i in Eq. (6) is fixed at the middle of the chain. One can clearly find the antiferromagnetic correlations between neighboring spins localized on one of the two-chains of the two-chain model, i.e., formation of the $2k_F$ spin-density-wave (SDW). One also notes that, because the charge fluctuations through the zigzag bonds connecting two chains are nearly zero due to a very small value of $t_1=t_2$, no spin correlations between two chains of the two-chain model are seen. As shown in the inset of Fig. 6(a), the spin-spin correlations decay as a power law, similar to those for the 1D Heisenberg chain, which depends very little on $V_2=t_2$ unless the $4k_F$ -CDW state is broken. This

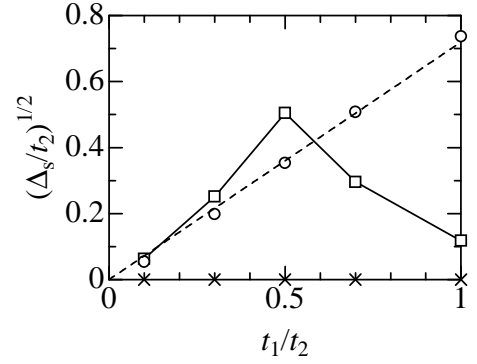


FIG. 7: Spin gap $\Delta_s=t_2$ as a function of $t_1=t_2$ for $V_2=t_2 = 0$ (crosses), 5 (squares), and 8 (open circles) at $V_1=t_2 = 5$ in the thermodynamic limit $L \rightarrow \infty$. The dashed line is $\Delta_s = 0.5(t_1=t_2)^2$.

suggests that the system may be well described as the 1D Heisenberg chain combined with an empty chain, as the in-line CO state may suggest.

Now let us turn to the correlations in the $2k_F$ -CDW phase (or the stripe-type CO phase in the two-chain notation). Fig. 6(b) shows the spin-spin correlation functions for $V_2=t_2 = 8$ and 10 at $V_1=t_2 = 5$. The behavior of $S(l)$ for $l = 4n$ ($n = 0; 1; 2; \dots$) shows the antiferromagnetic correlations. This corresponds to the $2k_F$ -SDW state of one of the two chains at quarter filling. We find simultaneously that there appears an SDW on the other chain; the phase of the SDW is shifted by $\pi/4$ from the other SDW. It might be as if the two SDW states coexist.

Because a sign of $S(4n)$ is opposite to those of $S(4n-1)$, the spins on the neighboring two sites should be opposite. The semi-log plot in the inset of Fig. 6(b) shows the exponential decay of the spin-spin correlations. The correlation lengths are 4.17 and 3.57 for $V_2=t_2 = 8$ and 10, respectively. $S(4n-1)$ and $S(4n-3)$, which correspond to the spin-spin correlations between two t_2 -chains, decay with the same correlation length as $S(4n)$. These behaviors are similar to the case of the two-leg Heisenberg (and half-filled Hubbard) ladder system. The correlation length is close to that for the two-leg isotropic Heisenberg system 3.19^{15} . This means the effective hopping between the next-nearest-neighbor sites along a t_2 -chain, i.e., sites i and $i+4$, is of the order of t_1 . Furthermore, we have found that $S(l)$ decays exponentially even in metallic regime near the $4k_F$ -CDW insulating phase.

From the exponential decay of the spin-spin correlations, we expect the system to be in a gapped spin-liquid state. In order to confirm it, we have calculated the spin gap defined by

$$\Delta_s(L) = E_0(N+1; N_{\#}-1; L) - E_0(N-1; N_{\#}+1; L) \quad (7)$$

for an L -site chain. In Fig. 7, we show the extrapolated values $\Delta_s (= \Delta_s(L \rightarrow \infty))$ at $V_1=t_2 = 5$ for $V_2=t_2 = 0$ ($4k_F$ -CDW phase), 5 (metallic phase), and 8 ($2k_F$ -CDW phase). In the $4k_F$ -CDW phase, we find that Δ_s is always zero, which is quite natural since the system can

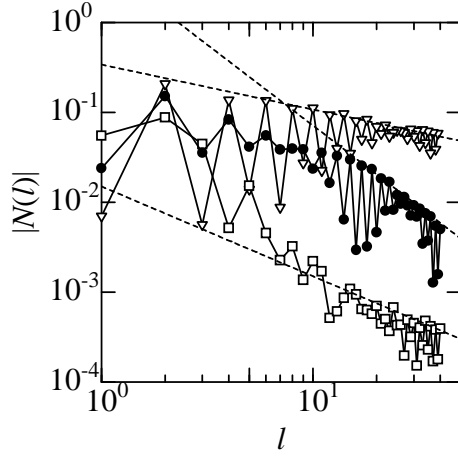


FIG. 8: Density-density correlation function $N(l)$ defined in Eq. (3) plotted on a log-log scale. The results are for $V_2=t_2 = 3$ (filled triangles), 4 (open squares), and 6 (filled circles) at $V_1=t_2 = 5$, with $L = 128$. The distance l is measured along the 1D chain of Fig. 1(c) in units of the interval between two sites.

be presumed to be a 1D Heisenberg model as mentioned above. In the $2k_F$ -CDW phase, we find that the spin gap is always finite except at $t_1 = 0$ and the size of the gap can be scaled with t_1^2 , i.e.,

$$\frac{s}{t_2} \sim \frac{1}{2} \frac{t_1}{t_2}^2; \quad (8)$$

as expected from the assumption that the neighboring two sites couple with the exchange interaction J . Because the spin gap for a two-leg isotropic Heisenberg ladder is $s = J/2$,¹⁵ we can estimate the effective exchange interaction as

$$\frac{J}{t_2} \sim \frac{t_1}{t_2}^2; \quad (9)$$

As for the metallic phase, s goes through a maximum at a finite value of $t_1=t_2$ because an increase of $t_1=t_2$ leads to an increase in the effective exchange coupling, as well as a decrease in the $2k_F$ -CDW fluctuations. This behavior reminds us of the spin gap of the two-leg CuO ladder materials where the gap behaves similarly as a function of the energy difference between the O and Cu sites.¹⁶

D. Luttinger parameter

Let us calculate the Luttinger parameter K which enables one to know competitions among correlations in the metallic phase. The Hamiltonian Eq. (1) has the energy dispersion relation

$$\epsilon(k) = 2t_1 \cos k - 2t_2 \cos 2k; \quad (10)$$

in the absence of interaction. If $t_1 = t_2$ and $n = \frac{1}{2}$, the Fermi surface has four Fermi points k_{F1} and k_{F2} , and

TABLE I: Calculated values of the Luttinger parameter K and charge velocity v_c at $V_1=t_2 = 5$.

$V_2=t_2$	K	v_c
2	0.55	0.295
3	1.25	0.738
4	0.88	0.401
5	0.27	< 0.01

even for finite interactions, one may expect that the system at low energies should behave as a two-band model.¹⁷ In the two-band model, it is known that only $4k_F$ -CDW and d-wave superconducting (SCd) correlations decay as power laws, and all other correlations decay exponentially; i.e., either SCd correlation or $4k_F$ -CDW correlation dominates for both weak and strong interactions.¹⁸ The $4k_F$ -CDW correlation and SCd correlation at large distances can be written like

$$N(l) \sim \cos(4k_F l) l^{-2K}; \quad (11)$$

and

$$h_{i+1}^y - h_i^y \sim l^{-1-2K}; \quad (12)$$

with

$$i = \frac{1}{2} (C_i - C_{i+1} + G_{\#} C_{i+1}); \quad (13)$$

respectively.

In Fig. 8, we show the density-density correlation function $N(l)$ defined in Eq. (3) on a log-log scale in order to estimate the exponent of the decay. At large distances ($l > 10$), the envelope of the correlation is consistent with a straight line on the log-log scale and therefore one may say that it decays as a power law. Fitting the decay to Eq. (11) allows us to determine the value of K although the fitting includes some errors due to Friedel oscillations in the data. The values obtained are given in Table I, which would be of sufficient accuracy when we consider available experimental results.

At $V_2=t_2 = 2.5$, $N(l)$ decays most rapidly and K is the largest. This means that the long-range interactions are effectively weakened since V_1 and V_2 are canceled with each other. Such a situation seems to be realized around $V_2=t_2 = V_1/(2t_2)$. Generally, long-range Coulomb repulsions suppress the value of K . In our results, K decreases when the values of V_1 and V_2 deviate from the relation $V_1 = 2V_2$, whereby the effective interaction strength increases. Now we note that the $2k_F$ -CDW transition occurs when $K = 1/4$, which may be understood if we suppose that two independent t_2 -chains at quarter filling undergo a $4k_F$ -CDW transition. On the other hand, the $4k_F$ -CDW transition occurs when $K = 1/2$. This may be understood if we assume that the system consists of a half-filled chain and an empty chain in the $4k_F$ -CDW phase.

We note that the SCd correlations decay more rapidly than the $4k_F$ -CDW correlations in the whole metallic phase even if $K > 1$. The inverse relationship of exponents predicted by a bosonization picture^{19,20} seems not to be preserved. The same situation was also seen for the two-leg Hubbard ladder,²¹ where it is known that enhancement of the SCd correlation is not adequately observed due to the finite-size effect, i.e., the widely separated energy levels near the Fermi energy.

The slopes at $l=L \rightarrow 0$ in Fig. 2(a) yield $v_c = (2K)^{-1}$, from which we can estimate the charge velocity v_c . We find that v_c goes through a maximum around $V_2 = t_2 = 2.5$ where the electrons can move almost freely despite the effect of double occupancy on a site. We note that the calculated very small charge velocities near the $2k_F$ - and $4k_F$ -CDW states (see Table I) may suggest heavy-Fermionic features, for which the geometrical frustration may play a crucial role.^{22,23,24}

E. Phase diagram

In Fig. 3 we show the ground-state phase diagram of the system in the parameter space of the intersite Coulomb interactions $V_1 = t_2$ and $V_2 = t_2$. The phases are distinguished by the presence of a gap for spin and/or charge excitations. Naturally, a CDW state is expected if either $V_1 = t_2$ or $V_2 = t_2$ is large. The ground state of the $2k_F$ -CDW ($4k_F$ -CDW) phase is a CO state with (without) spin gap and always insulating. Then, if both $V_1 = t_2$ and $V_2 = t_2$ are sufficiently small, the effective long-range Coulomb interaction is weak due to frustration between two interactions, the system may be in a metallic phase. The metallic phases can be divided into two regions. One is the spin-gapped-liquid (SGL) phase where there is a finite spin gap but no charge gap. Here, the system is under the influence of $2k_F$ -CDW transition and the $2k_F$ -CDW fluctuation is dominant. Another is the TLL phase where neither spin gap nor charge gap is present and the $4k_F$ -CDW fluctuation is dominant.

For a lucid discussion, let us now assume the case $U = t_2 \rightarrow 1$ and consider some limiting cases. When $V_1 = t_2 = 0$, the $2k_F$ -CDW transition occurs at $V_2 = t_2 \approx 2.3$. If the system can be regarded as two separate t_2 -chains due to very small $t_1 = t_2$, this transition would be equivalent to the $4k_F$ -CDW transition of the quarter-filled spinless Hubbard chain with the nearest-neighbor hopping t_2 and the next-nearest-neighbor Coulomb repulsion V_2 , where the critical value of $V_2 = t_2$ is expected to be 2, which is consistent with our results.

When $V_2 = t_2 = 0$, the $4k_F$ -CDW transition occurs around $V_1 = t_2 \approx 2$. We can estimate this value from comparison between the energies of the metallic and insulating solutions. First, the metallic solution may be obtained as follows. Consider the system consisting of two independent quarter-filled t_2 -chains. Then, if we assume the Coulomb repulsion between the t_2 -chains, the

total ground-state energy may roughly be evaluated as

$$2E_0^{t_2}(n = \frac{1}{2}) + \frac{V_1}{4}L : \quad (14)$$

Here $E_0^{t_2}(n = \frac{1}{2})$ is the ground-state energy of a spinless-Fermion model defined on a single chain at quarter filling with the nearest-neighbor hopping t_2 , and $V_1 = 4$ is the average Coulomb interaction. Next, the insulating solution may readily be obtained because it corresponds to the $4k_F$ -CDW state, i.e., one of the t_2 -chains is at half filling and another t_2 -chain is empty, whereby we obtain the ground-state energy to be almost zero. Hence, the condition for emergence of the $4k_F$ -CDW state is that the value of Eq. (14) is larger than zero. If we use an estimation $E_0^{t_2}(n = \frac{1}{2}) \approx 0.25t_2L$ made from the Lieb-Wu equations,²⁵ the critical interaction strength can be obtained as $V_1 = t_2 \approx 2$. We should note that, because we have used a small but finite value of $t_1 = t_2$, the actual critical values of the interactions calculated are rather larger than the above estimation.

Next, we turn to the case where both $V_1 = t_2$ and $V_2 = t_2$ are nonzero. Naturally, the system is metallic for small V_1 and V_2 (< 0 (t_2)), and the metallic phase becomes narrower as the long-range Coulomb interactions increase along the line $V_2 = t_2 = V_1 = (2t_2)$. For very large values of V_1 and V_2 , the boundary between the $2k_F$ -CDW (the $4k_F$ -CDW) and the SGL (TLL) phases becomes parallel to the line $V_2 = t_2 = V_1 = (2t_2)$, and the distance between the two phases remains to be of the order of t_2 (t_1) even in the limit of $V_1 \rightarrow 1$ and $V_2 \rightarrow 1$. Even if there is no hybridization, i.e., $t_1 = t_2 = 0$, the charge mode is gapless on the line $V_2 = t_2 = V_1 = (2t_2)$. This means that the effects of V_1 and V_2 are precisely cancelled out on that line. Now, if finite values of t_1 and/or t_2 are introduced, the energy gain due to moving holes expands the width of the line. We point out that the width of metallic regime depends on the difference V between two repulsive interactions V_1 and V_2 ($V = V_1 - V_2$), rather than the values V_1 and V_2 themselves. To check this notion, we calculate the critical strength of $V_2 = t_2$ for very large value of $V_1 = t_2$. The critical interaction strengths for the $4k_F$ -CDW and $2k_F$ -CDW transitions are obtained respectively as follows: $V_2 = t_2 \approx 249.5$ and 253.5 for $V_1 = t_2 = 500$, and $V_2 = t_2 \approx 499.5$ and 503.5 , where we assume $V_1 = t_2 = 1000$ and $U = t_2 = 4000$. If $t_1 = 0$ ($t_2 = 0$), the boundary of the $2k_F$ -CDW (the $4k_F$ -CDW) phase should be asymptotic to the line $V_2 = t_2 = V_1 = (2t_2)$.

IV. SUMMARY AND DISCUSSION

Using the DMRG method, we have studied the electronic states of a two-chain Hubbard model at quarter filling that models the low-energy electronic states of the CuO double chains of $\text{PrBa}_2\text{Cu}_4\text{O}_8$. We have shown that the model has the CO phases with the stripe-type and in-line-type patterns in the parameter space and between

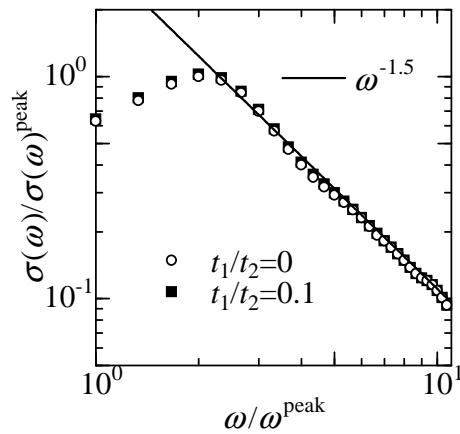


FIG. 9: Normalized optical conductivity on a log-log scale. Parameter values used for calculation are: $U=t_2 = 20$, $V_1=t_2 = 2$, $V_2=t_2 = 5$, $L = 32$, and $n = 0.46875$. Finite broadening width $\gamma = 0.4t_2$ is introduced. The solid line shows a fitting to the form $(\omega/\omega_{\text{peak}})^{-1.5}$. A slope of -1.5 is found.

the two CO phases there appears a wide region of vanishing charge gap, which is due to geometrical frustration of the long-range Coulomb interactions. The phase diagram of our model consists of four phases characteristic of (i) the stripe-type CO (or $2k_F$ -CDW), (ii) in-line (type CO (or $4k_F$ -CDW), (iii) Tomonaga-Luttinger liquid, and (iv) spin-gapped liquid. For the liquid phases, we have suggested possible emergence of a heavy-Fermion-like behavior, which can occur near the region of the metal-insulator phase boundary.

Finally, let us discuss consistency between our numerical results and available experimental data on $\text{PrBa}_2\text{Cu}_4\text{O}_8$. Comparable experimental features are the appearance of the TLL behaviors and estimation of the value $K \approx 0.24$ ^{5,7,8}. We can explain such a small value of K only by assuming that the system is in the $2k_F$ -CDW state or in the SGL state near the $2k_F$ -CDW phase boundary. In these two phases of our phase diagram, however, a small but finite spin gap clearly exists except at $t_1 = 0$. We have also confirmed that the spin gap remains open even if the system is doped slightly away from quarter filling. Thus, the phase is not TLL unless $t_1 = 0$, which is apparently not consistent with experiment. One possibility for reconciliation may be that the CuO double chain system has a very small value of

t_1 , so that experiments performed with finite resolution cannot detect the effects of the spin gap. Another possibility is that the optical and ARPES spectra observed in relatively high energies are insensitive to the opening of the spin gap. To demonstrate this, we have calculated the optical conductivity of our model with the dynamical DMRG method²⁶ and confirmed that the shape of the higher energy part ($\hbar\omega > \Delta_c$) of the conductivity does not depend on the existence of small values of t_1 . In Fig. 9, we show an example of the t_1 -dependence of the optical conductivity calculated for a possible set of parameters. We find that the spectra for $t_1=t_2 = 0$ and 0.1 are almost the same and the power-law decay can be seen at $\hbar\omega > \Delta_c$. From a fit of the results to the form

$(\omega/\omega_{\text{peak}})^{-\alpha}$, we estimate the value $\alpha \approx 1.5$, which corresponds to $K \approx 0.22$. This value is very close to the value obtained experimentally. Here we point out that the long-range CDW ground state cannot reproduce the experimental spectrum but a small hole doping of only a few % changes the shape of spectrum largely leading to the power-law decay of the spectra at high energies. We therefore suggest that the actual material is located in the SGL phase near the $2k_F$ -CDW phase or in the $2k_F$ -CDW phase with slight doping. We also want to suggest that, if the NMR Knight-shift measurement is made on the spin degrees of freedom of the double-chain $\text{Cu}(1)$ site of $\text{PrBa}_2\text{Cu}_4\text{O}_8$, one should be able to detect anomalous behaviors associated with the spin-singlet formation due to the stripe-type fluctuation of charge carriers.

Acknowledgments

We would like to thank E. Jeckelmann for the use of the DMRG code originally written by him and useful discussions on the numerical techniques. We also would like to thank S. Fujiyama, H. Ikuta, Y. Itoh, and K. Takenaka for enlightening discussion on the experimental aspects. This work was supported in part by Grants-in-Aid for Scientific Research (Nos. 11640335 and 12046216) from the Ministry of Education, Culture, Sports, Science, and Technology of Japan. A part of computations was carried out at the computer centers of the Institute for Molecular Science, Okazaki, and the Institute for Solid State Physics, University of Tokyo.

Electronic address: sato@physik.uni-mainz.de

^y Electronic address: ohta@science.s.chiba-u.ac.jp

¹ S. Horii, U. Mizutani, H. Ikuta, Y. Yamada, J. H. Ye, A. Matsushita, N. E. Hussey, H. Takagi, and I. Hirabayashi, Phys. Rev. B 61, 6327 (2000).

² S. Horii, H. Takagi, H. Ikuta, N. E. Hussey, I. Hirabayashi, and U. Mizutani, Phys. Rev. B 66, 054530 (2002).

³ N. E. Hussey, M. N. M. cBrien, L. B. Falicov, J. S. Brooks, S.

H. Horii, and H. Ikuta, Phys. Rev. Lett. 89, 086601 (2002).

⁴ S. Fujiyama, M. Takigawa, and S. Horii, Phys. Rev. Lett. 90, 147004 (2003).

⁵ K. Takenaka, K. Nakada, A. Ohsuka, S. Horii, H. Ikuta, I. Hirabayashi, S. Sugai, and U. Mizutani, Phys. Rev. Lett. 85, 5428 (2000).

⁶ R. Fehrenbacher and T. M. Rice, Phys. Rev. Lett. 70, 3471 (1993).

⁷ T. Mizokawa, A. Ino, T. Yoshida, A. Fujimori, C. Kim,

- H. Eisaki, Z.-X. Shen, S. Horii, T. Takeshita, S. Uchida, K. Tomimoto, S. Tajima, and Y. Yamada, in *Stripes and Related Phenomena*, edited by A. Bianconi and N. L. Saini (Plenum, New York, 2000).
- ⁸ T. Mizokawa, K. Nakada, C. Kim, Z.-X. Shen, T. Yoshida, A. Fujimori, S. Horii, Y. Yamada, H. Ikuta, and U. Mizutani, *Phys. Rev. B* **65**, 193101 (2002).
- ⁹ H. Seo and M. Ogata, *Phys. Rev. B* **64**, 113103 (2001).
- ¹⁰ A. K. Zhuravlev, M. I. Katsnelson, and A. V. Trelov, *Phys. Rev. B* **56**, 12939 (1997); A. K. Zhuravlev and M. I. Katsnelson, *ibid.* **61**, 15534 (2000).
- ¹¹ R. Amasaki, Y. Shibata, and Y. Ohta, *Phys. Rev. B* **66**, 012502 (2002); .
- ¹² S. R. White, *Phys. Rev. Lett.* **69**, 2863 (1992); *Phys. Rev. B* **48**, 10345 (1993).
- ¹³ For an example of this procedure, see J. Bonca, J. E. Gubematics, M. Guerrero, E. Jeckelmann, and S. R. White, *Phys. Rev. B* **61**, 3251 (2000).
- ¹⁴ H. Yoshioka, M. Tsuchiizu, and Y. Suzumura, *J. Phys. Soc. Jpn.* **70**, 762 (2001).
- ¹⁵ S. R. White, R. M. Noack, and D. J. Scalapino, *Phys. Rev. Lett.* **73**, 886 (1994).
- ¹⁶ S. Nishimoto, E. Jeckelmann, and D. J. Scalapino, *Phys. Rev. B* **66**, 245109 (2002).
- ¹⁷ M. Fabrizio, *Phys. Rev. B* **54**, 10054 (1996).
- ¹⁸ H. J. Schulz, *Phys. Rev. B* **53**, R2959 (1996).
- ¹⁹ L. Balents and M. P. A. Fisher, *Phys. Rev. B* **53**, 12133 (1996).
- ²⁰ N. Nagaosa and M. Oshikawa, *J. Phys. Soc. Jpn.* **65**, 2241 (1996); N. Nagaosa, *Solid State Commun.* **94**, 495 (1995).
- ²¹ R. M. Noack, S. R. White, and D. J. Scalapino, *Physica C* **270**, 281 (1994).
- ²² M. Shiga, H. Wada, Y. Nakamura, J. Deportes, and K. R. A. Ziebeck, *J. Phys. Soc. Jpn.* **57**, 3141 (1988); M. Shiga, K. Fujisawa, and H. Wada, *ibid.* **62**, 1329 (1993).
- ²³ S. Kondo, D. C. Johnston, C. A. Swenson, F. Borsa, A. V. Mahajan, L. L. Miller, T. Gu, A. I. Goldman, M. B. Maple, D. A. Gajewski, E. J. Freeman, N. R. Dilley, R. P. Dickey, J. Merrin, K. Kojima, G. M. Luke, Y. J. Uemura, O. Chmaisson, and J. D. Jorgensen, *Phys. Rev. Lett.* **78**, 3729 (1997).
- ²⁴ S. Fujimoto, *Phys. Rev. B* **64**, 085102 (2001).
- ²⁵ E. H. Lieb and F. Y. Wu, *Phys. Rev. Lett.* **20**, 01445 (1968).
- ²⁶ E. Jeckelmann, *Phys. Rev. B* **66**, 045114 (2002).